Hsp110 mitigates α-synuclein pathology in vivo

Yumiko V. Taguchi[a], Erica L. Gorenberg[a], Maria Nagy[b], Drake Thrasher[c], Wayne A. Fenton[b], Laura Volpicelli-Daley[c], Arthur L. Horwich[b,d], and Sreeganga S. Chandra[a,e,f,1]

[a]Department of Neurology, Yale University, New Haven, CT 06536; [b]Howard Hughes Medical Institute, Yale University, New Haven, CT 06510; [c]Department of Neurology, University of Alabama, Birmingham, AL 35294; [d]Department of Genetics, Yale University, New Haven, CT 06510; [e]Department of Neuroscience, Yale University, New Haven, CT 06536; and [f]Yale Stem Cell Center, Yale University, New Haven, CT 06510

Edited by Solomon H. Snyder, Johns Hopkins University School of Medicine, Baltimore, MD, and approved October 14, 2019 (received for review February 24, 2019)

Parkinson's disease is characterized by the aggregation of the presynaptic protein α-synuclein and its deposition into pathologic Lewy bodies. While extensive research has been carried out on mediators of α-synuclein aggregation, molecular facilitators of α-synuclein disaggregation are still generally unknown. We investigated the role of molecular chaperones in both preventing and disaggregating α-synuclein oligomers and fibrils, with a focus on the mammalian disaggregase complex. Here, we show that overexpression of the chaperone Hsp110 is sufficient to reduce α-synuclein aggregation in a mammalian cell culture model. Additionally, we demonstrate that Hsp110 effectively mitigates α-synuclein pathology in vivo through the characterization of transgenic Hsp110 and double-transgenic α-synuclein/Hsp110 mouse models. Unbiased analysis of the synaptic proteome of these mice revealed that overexpression of Hsp110 can override the protein changes driven by the α-synuclein transgene. Furthermore, overexpression of Hsp110 is sufficient to prevent endogenous α-synuclein templating and spread following injection of aggregated α-synuclein seeds into brain, supporting a role for Hsp110 in the prevention and/or disaggregation of α-synuclein pathology.

Lewy body | chaperone | synapse | proteomics | disaggregase

Parkinson's disease (PD) is a progressive neurodegenerative disease affecting roughly 1% of the population over 65 y old (1). PD is characterized by the aberrant aggregation of α-synuclein, a presynaptic protein involved in synaptic vesicle trafficking (2–5). Fibrillized α-synuclein is the major component of Lewy bodies, the aggregative hallmark pathology of PD (6). The discovery of several point mutations (A53T, A53E, A30P, E46K, G51D) (7–12), duplications, and triplication of the α-synuclein gene *SNCA* (13, 14) resulting in autosomal dominant PD have cemented α-synuclein's integral role in PD pathophysiology. The *SNCA* point mutations and multiplications exert their effects through increased protein aggregation. Interestingly, several other neurodegenerative diseases, such as Lewy body dementia, also exhibit α-synuclein pathology and are classified as synucleinopathies. Strategies to prevent and alleviate α-synuclein aggregation are therefore crucial to generating effective therapeutics for the treatment of PD and other synucleinopathies.

Heat shock protein 70 (Hsp70) proteins are the mainstay class of chaperones that assist in protein folding (15). Constitutive Heat shock cognate 70 (Hsc70) as well as its inducible form, Hsp70, recognize hydrophobic residues of newly synthesized or misfolded proteins, binding transiently in a cyclic, ATP-dependent manner to mediate protein (re)folding (16, 17). Hsp70 activity is facilitated by 2 classes of cochaperones: DnaJ proteins, which recruit appropriate substrates and accelerate Hsp70 ATPase activity, and a nucleotide exchange factor (NEF), which promotes ADP and P_i release and ATP binding to the Hsp70 (18–22). Together, Hsc70 and Hsp70 facilitate proper protein folding and, importantly, prevent protein misfolding.

Recent studies have identified the mammalian Hsp70 disaggregase, a chaperone complex involved in the disaggregation of proteins from insoluble aggregates (23, 24), akin to Hsp104 and ClpB found in nonmetazoans (25). This complex consists of Hsp70, Hsp110, DnaJA, and DnaJB proteins. Subsequently, Gao et al. (26) described a related Hsc70 complex capable of breaking down α-synuclein fibrils in vitro. By reconstituting the disaggregase with purified proteins, this complex was shown to release soluble monomeric α-synuclein from its fibrillized form. The α-synuclein fibril-specific disaggregase complex is composed of Hsc70, the DnaJ protein DnaJB1, and NEF Hsp110 in the molar ratio 1.0:0.5:0.1 (26–29). DnaJB1 binds α-synuclein fibrils, recruiting Hsc70 to the surface of aggregates and promoting ATP hydrolysis, while Hsp110 accelerates the rate-limiting step of nucleotide exchange—the release of ADP and P_i followed by ATP binding. The release of ADP was shown to cause a power stroke responsible for fibril disassembly through a combination of fibril fragmentation and depolymerization (26).

Although the Hsc70 disaggregase complex can reverse α-synuclein aggregation in vitro, the effects of this complex on α-synuclein aggregation in vivo have not been assessed. In neurons, Hsc70 is the most abundant molecular chaperone and is constitutively expressed, while DnaJB1 and Hsp110 are present at relatively low levels (30). Thus, increasing either DnaJB1 or Hsp110 are reasonable options to enhance disaggregase activity in the brain (31, 32). Recently, Hsp110 was implicated as the limiting factor in the Hsc70-DnaJB1-Hsp110 disaggregase complex (24, 31). Furthermore, the Hsp110 knockout mouse exhibits age-dependent protein aggregation in the brain (33). Conversely, in a study focusing on disaggregase activity in a SOD1-linked amyotrophic lateral sclerosis (ALS) mouse model, Hsp110 overexpression significantly improved the survival of ALS mice, increasing mean survival by 2 mo (31). Hence, we opted to overexpress Hsp110

Significance

Recently, the mammalian disaggregase that can disassemble α-synuclein fibrils was reconstituted in vitro. However, it was unclear if this disaggregase can function in vivo. Here we show that overexpressing Hsp110, a limiting component of the disaggregase, is beneficial in reducing α-synuclein fibrillar pathology in 2 distinct mouse models of Parkinson's disease. This reduction in α-synuclein pathology leads to improved survival. Significantly, Hsp110 overexpression is associated with a broad elevation of chaperones and may be an effective therapeutic strategy against synucleinopathies.

Author contributions: Y.V.T., W.A.F., L.V.-D., A.L.H., and S.S.C. designed research; Y.V.T., E.L.G., M.N., D.T., and L.V.-D. performed research; Y.V.T., E.L.G., L.V.-D., A.L.H., and S.S.C. analyzed data; and Y.V.T., E.L.G., W.A.F., L.V.-D., A.L.H., and S.S.C. wrote the paper.

The authors declare no competing interest.

This article is a PNAS Direct Submission.

Data deposition: The data reported in this article have been deposited in the PRIDE database, https://www.ebi.ac.uk/pride/archive/ (accession no. PXD016015).

[1]To whom correspondence may be addressed. Email: sreeganga.chandra@yale.edu.

This article contains supporting information online at www.pnas.org/lookup/suppl/doi:10.1073/pnas.1903268116/-/DCSupplemental.

First published November 4, 2019.

to investigate whether the disaggregase can prevent or reverse α-synuclein pathology in vivo.

Previous unbiased proteomic studies of Lewy bodies from patient brains have shown an enrichment of Hsc70, DnaJB1, and Hsp110 (34), suggesting that the disaggregase does recognize misfolded α-synuclein but is insufficient to prevent its aggregation. Here we show that overexpression of Hsp110 both in mammalian culture and in transgenic mice (31) ameliorates α-synuclein aggregation in vivo. We also observe strong protective effects of Hsp110 overexpression in α-synuclein spread. Together, these experiments strongly support an ameliorative role for Hsp110 in vivo and indicate that enhancement of Hsp110 levels could be of benefit for PD and other synucleinopathies.

Results

Hsp110 Overexpression Ameliorates α-Synuclein Aggregation in Mammalian Culture. To establish that the α-synuclein fibril-disaggregase complex functions in a cellular context, we utilized an α-synuclein seeding assay in HEK293T cells that produces visible cytosolic aggregates (35, 36). First, HEK293T cells were transfected with human α-synuclein–GFP with or without Hsp110 (HspA4L/Apg1/Hsph3) constructs, which results in a 51.6- ± 6.1-fold increase in α-synuclein and a 3.7- ± 0.51-fold increase in Hsp110 protein levels (Fig. 1 *B* and *C*). Following Hsp110 and α-synuclein–GFP overexpression, aggregated recombinant human untagged α-synuclein seeds (Fig. 1*A*) were added to the media to induce cytosolic aggregation. Cells were washed and cellular α-synuclein aggregate levels were assessed by Western blotting (35, 36). Consistent with our previous results (36), the addition of α-synuclein seeds resulted in a significant amount of high molecular weight (HMW) α-synuclein by Western blot (Fig. 1 *B* and *D*). When Hsp110 was co-overexpressed, these HMW α-synuclein species were significantly reduced by ∼50% (1.0 versus 0.48; $P = 0.0003$). Next, we immunostained the treated HEK293T cells and assessed the effects of Hsp110 overexpression on GFP-positive aggregates by confocal microscopy. We found that Hsp110 overexpression resulted in ∼50% fewer GFP-positive aggregates (14 versus 8% cells; $P = 0.003$; Fig. 1 *E* and *F*), suggesting that the additional Hsp110 was increasing a putative disaggregase activity, the action of which disassembled α-synuclein seeds or intracellular GFP-positive aggregates or both. These results suggest that Hsp110 overexpression is an effective strategy to mitigate α-synuclein aggregation.

Hsp110 Transgenic Overexpression Enhances Proteostasis Capacity In Vivo. To characterize the effectiveness of Hsp110 overexpression in vivo, we utilized Thy-1 Hsp110 transgenic mice, which have been described in the context of a mouse model of ALS (31). We began by quantifying the levels of Hsp110 protein in brain and spinal cords of wild-type (WT) and transgenic mice. We established that Hsp110 levels were increased 2.06- ± 0.03-fold in brain homogenates ($P < 0.05$) and 1.95- ± 0.15-fold in spinal cord homogenates ($P < 0.05$) in transgenics (Fig. 2 *A* and *B*), consistent with a previous publication (31). We also immunoblotted for Hsc70 and DnaJB1, the 2 other α-synuclein putative disaggregase components and found elevated levels of Hsc70 (1.51- ± 0.14-fold in brain, $P = 0.006$; 1.55- ± 0.15-fold in spinal cord, $P = 0.07$), but not of DnaJB1, in both the brain and spinal cord of Hsp110 transgenic mice (Fig. 2 *A* and *B*). Thus, based on the in vitro stoichiometry of the WT disaggregase (Hsc70:DnaJB1:Hsp110::1:0.5:0.1) and assuming that DnaJB1 levels are not limiting, these increases could double the disaggregase activity in vivo.

The increase in Hsc70 levels in Hsp110 transgenic brains was unexpected, so we evaluated if overexpression of Hsp110 was leading to a broad enhancement of chaperone levels and hence proteostasis capacity by unbiased label-free quantification (LFQ) mass spectrometry. We chose to examine the synaptic proteome as α-synuclein is normally localized within presynaptic termini

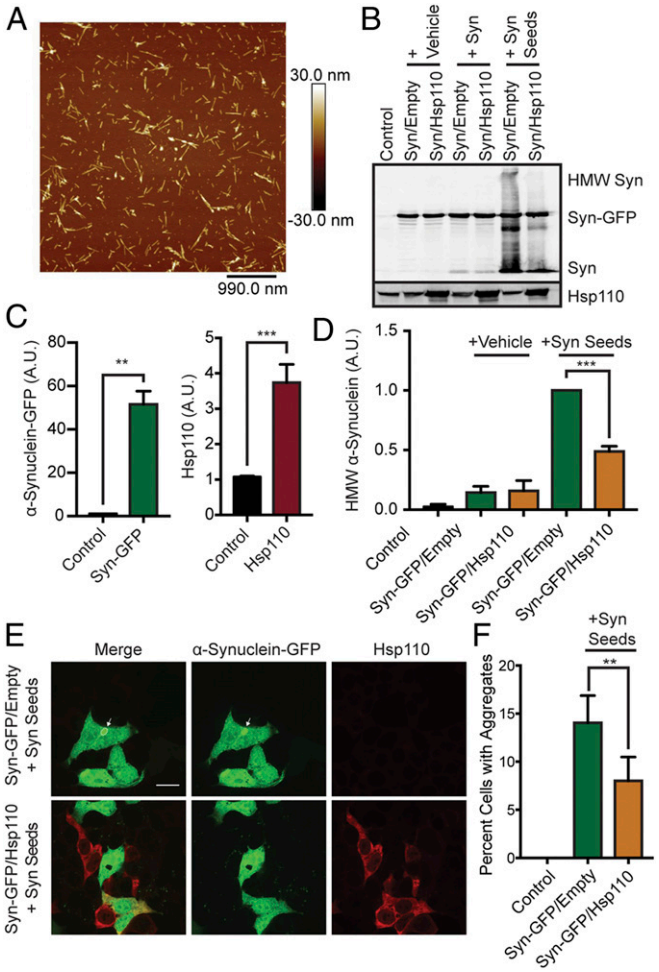

Fig. 1. Hsp110 overexpression in mammalian cells alleviates α-synuclein aggregation. (*A*) Atomic force microscopy showing morphology of α-synuclein oligomers (Syn seeds). (*B*) Western blot of HEK293T cells overexpressing α-synuclein–GFP or both α-synuclein–GFP and Hsp110 treated with vehicle, α-synuclein fibrils (Syn), or α-synuclein oligomers (Syn seeds). HMW α-synuclein is indicative of internalization of seeds and intracellular α-synuclein aggregation. (*C*) Quantification of α-synuclein–GFP and Hsp110 overexpression in HEK293T Western blot, shown in *B*. (*D*) Quantification of HMW α-synuclein in HEK293T Western blot, shown in *B*. $n = 3$ experiments per condition. (*E*) Representative images of HEK293T cells transfected with α-synuclein–GFP (green) and Hsp110 (red) following α-synuclein aggregate addition. (Scale bar, 10 μm applies to all panels.) A GFP-positive α-synuclein aggregate is indicated by a white arrow. (*F*) Quantification of the percentage of GFP-positive HEK293T cells with intracellular GFP-positive aggregates templated from added α-synuclein seeds. Two-tailed Student *t* test: $n = 6$/condition; $^{**}P < 0.01$; $^{***}P < 0.001$.

(37) and its aggregation is initiated there. We evaluated the synaptic proteomes from WT and Hsp110 transgenic mice and confirmed that Hsp110 and Hsc70 levels increased (5.92- ± 1.5-fold for Hsp110 and 1.9- ± 0.32-fold for Hsc70), but that of DnaJB1 did not, which is similar to the whole-brain Western blotting data (Fig. 2 *A* and *B*). Comparing LFQ mass spectrometry quantifications suggests that Hsp110 is in fact enriched relative to Hsc70 at synaptic termini in Hsp110 transgenics compared to the WT (Fig. 2*C*). In addition, the LFQ analysis revealed a significant increase in other members of the Hsp70 family, such as HspA1a, HspA2, HspA12a, and Hsp72, as well as Hsp40 family members, including DnaJA1 and DnaJC5 (Fig. 2*C* and *SI Appendix*, Fig. S1*C*). There were also modest increases for Hsp105 (HspH1) and Hsp90s (Fig. 2*C*). Hence, Hsp110 overexpression can broadly enhance proteostasis capacity.

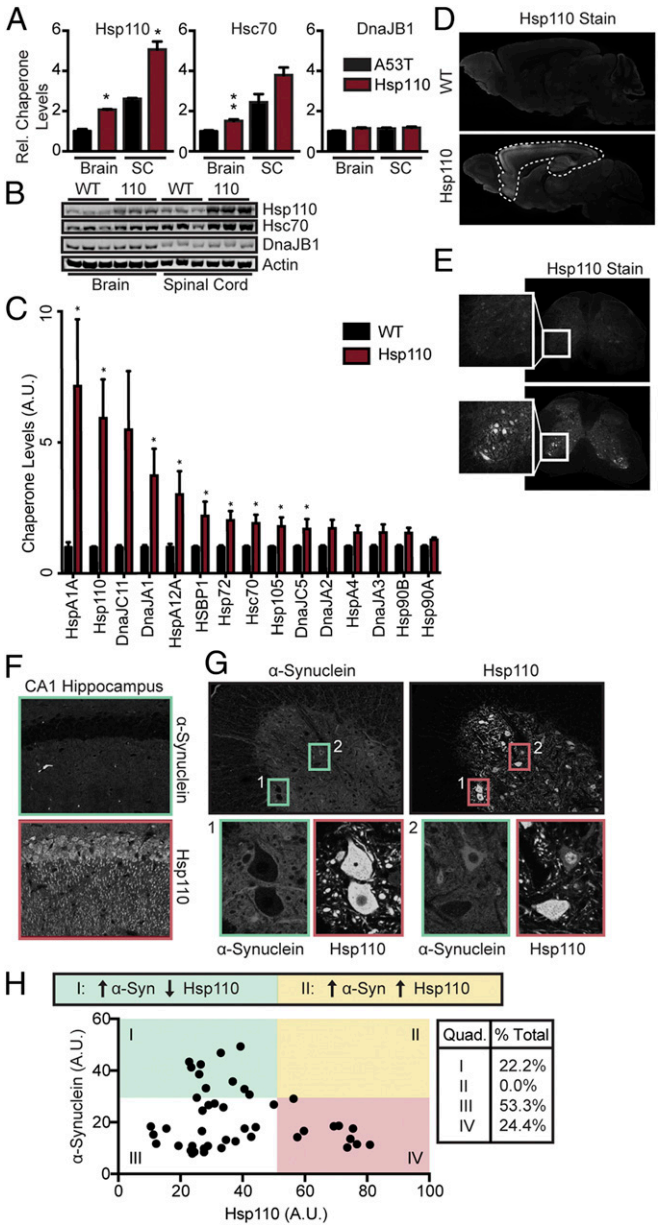

Fig. 2. Characterization of Hsp110 transgenic mouse line. (*A* and *B*) Western blot and quantitation of Hsp110, Hsc70, and DnaJB1 expression levels in whole mouse brain and spinal cord at 6 mo ($n = 3$/genotype). (*C*) Quantification of chaperone levels in WT and Hsp110 transgenics by LFQ mass spectrometry ($n = 3$ biological replicates, 3 technical replicates; at 6 mo). (*D*) Immunohistochemistry of WT and Hsp110 mouse brain stained for Hsp110 at 6 mo. Hsp110 mice show strong Hsp110 overexpression in the hippocampus, cortex, and anterior olfactory nucleus. Mild overexpression is observed in the thalamus and caudate putamen. (*E*) Immunohistochemistry of WT and Hsp110 mouse spinal cord stained for Hsp110 at 6 mo. (*Inset*) Ventral horn depicts strong somatic Hsp110 expression in motor neurons. (*F*) Immunohistochemistry of WT and Hsp110 mouse hippocampus stained for Hsp110 at 6 mo. (*G*) Representative fluorescence images of the ventral horn of L2 of the spinal cord of 6-mo-old Hsp110-overexpressing mice, stained with α-synuclein (*Left*, green channel) and Hsp110 (*Right*, red channel). α-Synuclein exposure has been artificially increased in the *Left* image to allow for easier viewing. Two representative images of neurons are enlarged in both channels. *Inset* 1 depicts an example of motor neurons with low somatic α-synuclein and high somatic Hsp110 levels (quadrant IV in *H*), while *Inset* 2 depicts an example of a motor neuron with high somatic α-synuclein and low somatic Hsp110 (quadrant I in *H*). (*H*) Scatterplot illustrating somatic α-synuclein and Hsp110 levels in each motor neuron assessed. A mild inverse relationship was found (slope = –0.35, $R^2 = 0.22$), with no high-fluorescing Hsp110 cells also expressing high levels of α-synuclein.

Next, WT and transgenic brain and spinal cord sections were immunostained for Hsp110. The immunostaining pattern revealed overexpression in cortex, hippocampus, and anterior olfactory nucleus (Fig. 2*D*), while in spinal cord, Hsp110 was selectively enriched in motor neurons (Fig. 2*E*). To test if Hsp110 overexpression impacts endogenous α-synuclein, we surveyed somatic α-synuclein in CA1 pyramidal neurons of hippocampus and within motor neurons of 6-mo-old Hsp110 transgenic mice (Fig. 2 *F*–*H*). α-Synuclein is a presynaptic protein (37), but relocalizes to the soma with protein aggregation and aging (38). We observed somatic expression of α-synuclein occasionally in aged spinal cord (Fig. 2*G*) but not in aged hippocampus (Fig. 2*F*; 6 mo) using a pan α-synuclein antibody, consistent with previous literature (38). By quantifying somatic α-synuclein and Hsp110 levels in spinal motor neurons, we saw that they were slightly inversely correlated (Fig. 2*H*). In particular, while α-synuclein levels were variable in neuronal soma with low levels of Hsp110, α-synuclein levels were consistently low (<30 arbitrary units [A.U.]) in neuron soma with high levels of Hsp110 (Fig. 2*H*), suggesting that increased levels of Hsp110 inhibit α-synuclein accumulation in the soma. This is made more evident by dividing the graph in Fig. 2*H* into quadrants. In quadrants I and III (pale green, white), where somatic Hsp110 levels were relatively low, 75% of neuronal soma had α-synuclein. In contrast, in quadrant II (pale yellow), where Hsp110 levels were 2- to 4-fold higher, no neurons with somatic α-synuclein accumulations above 30 A.U. were observed. These findings suggest that transgenic overexpression of Hsp110 could be beneficial in terms of α-synuclein accumulation and that there is a threshold for the ratio of Hsp110 to α-synuclein above which overexpression becomes effective.

Double Transgenics of α-Synuclein and Hsp110 to Investigate Disaggregase In Vivo. The transgenic human α-synuclein A53T mouse line is a well-characterized model of α-synucleinopathy and PD (39, 40). This line exhibits α-synuclein pathology and develops motor symptoms starting at 6 mo of age (39, 41). To test if Hsp110 overexpression is effective against α-synucleinopathy in vivo, we crossed the Hsp110 mice with the α-synuclein A53T line to generate mice with the following genotypes: WT, Hsp110, A53T, and Hsp110/A53T (110A53T). Western blotting of brain and spinal cord extracts from these mice for disaggregase components showed that Hsp110 and Hsc70 levels were increased in Hsp110 mice as previously observed (Fig. 2 *A* and *B*) and slightly further increased in 110A53T animals (*SI Appendix*, Fig. S1 *A* and *B*), while DnaJB1 levels were unaltered in all genotypes. Both the A53T and 110A53T lines show elevated α-synuclein levels in brain and spinal cord (~3.2-fold; *SI Appendix*, Fig. S1 *A* and *B*), suggesting that Hsp110 expression is largely not altering α-synuclein expression.

To evaluate whether transgenic Hsp110 ameliorates the pathogenic effects of α-synuclein overexpression, we performed unbiased LFQ mass spectrometry. We compared the profiles of 110A53T to those of A53T and Hsp110 each relative to WT (Fig. 3 and *SI Appendix*, Fig. S2; $n = 1{,}556$ proteins). As seen in Fig. 3*A*, A53T samples show a large alteration in relative protein expression compared to 110A53T (slope = 0.606 ± 0.006). Significantly, the Hsp110 profile looks similar to the 110A53T profile (slope = 0.844 ± 0.006), strongly suggesting that Hsp110 overexpression reverses the overall proteomic changes seen in A53T samples. This is further evident when examining individual proteins by plotting their relative changes as a heat map (Fig. 3*B*) or volcano plot

$n = 45$ cells. Quadrants are defined with an α-synuclein threshold of 30 A.U. and Hsp110 threshold of 50 A.U. All Hsp110 motor neurons fall in quadrants I, III, and IV, while no neurons fall in quadrant II, suggesting that high expression of Hsp110 prevents somatic relocation of α-synuclein. $n = 3$ to 4 mice/genotype; $^*P < 0.05$; $^{**}P < 0.01$. Data analyzed by Student's *t* test in *C*.

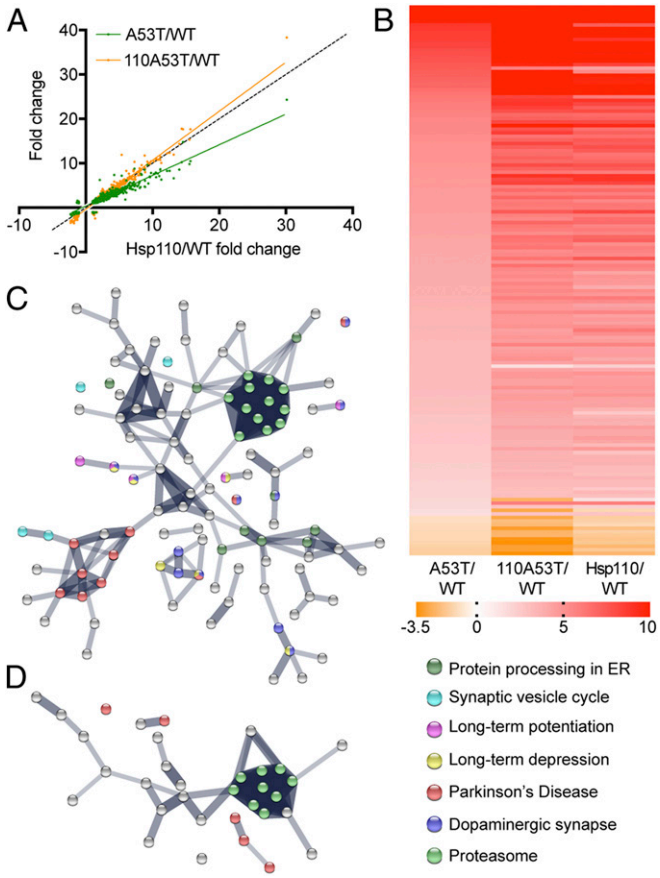

Fig. 3. Proteomic analysis of 110A53T, A53T, and Hsp110 brains. (*A*) Synaptic protein expression levels in 110A53T were plotted against those in A53T and Hsp110 after normalization to WT. Confidence interval for slope of the line for A53T = 0.606 ± 0.006 while slope of the line for Hsp110 = 0.844 ± 0.00611. Dotted line indicates $x = y$. (*B*) Heatmap of protein expression changes in A53T, Hsp110, and 110A53T as compared to WT. The expression levels of 142 proteins with a >1-fold change difference in A53T/WT versus 110A53T/WT are shown here in order of decreasing A53T/WT ratio. Red indicates a 10-fold change or greater, orange indicates a −3.5-fold change or less, and white indicates no change. (*C*) STRING analysis of differences between A53T and 110A53T. (*D*) STRING analysis of differences between Hsp110 and 110A53T. $n = 3$ biological, 3 technical replicates. Mice were 6 mo old.

(*SI Appendix*, Fig. S2). The Hsp110 expression pattern is similar to the 110A53T but not to the A53T pattern. This is likely in part because the elevated chaperone levels seen in Hsp110 transgenics (Fig. 2*C*) persist in 110A53T transgenics (*SI Appendix*, Fig. S1*C*). To understand which pathways are impacted in these mouse lines, we input the proteins that had a greater than 1-fold expression difference between A53T and 110A53T (Fig. 3*C*) or between Hsp110 and 110A53T (Fig. 3*D*) to STRING analysis. This analysis revealed that several of the pathways related to PD and proteasomal degradation were altered in the A53T vs. 110A53T comparison (Fig. 3*C*) while fewer changes to these pathways were identified in the Hsp110 vs. 110A53T comparison (Fig. 3*D*). Taken together, Hsp110 overexpression appears to be reversing some of the protein expression changes seen in the A53T α-synuclein model of PD.

We assessed if Hsp110 overexpression ameliorates aggregative α-synuclein pathology in vivo in aged littermate cohorts of WT, Hsp110, A53T, and 110A53T mice. We first tested if Hsp110 overexpression impacted somatic accumulation of α-synuclein in the context of transgenic overexpression at 6 mo. As seen in Fig. 4*A*, WT and Hsp110 transgenic mice do not show any notable accumulation of α-synuclein in the cell bodies of pyramidal CA1 neurons, similar to Fig. 2*F*. However, A53T sections have high levels of somatic α-synuclein in these neurons, while neurons in 110A53T sections have lower amounts (355.47 ± 21 A.U. in A53T versus 236.3 ± 15 A.U. in 110A53T; $P < 0.0001$). Similar results for synaptic α-synuclein levels were observed in the 4 strains (Fig. 4 *A* and *B*). We next immunostained for pSer129–α-synuclein, a bona fide marker of fibrillized α-synuclein pathology in both patients and rodent models of PD (42, 43). Imaging of the CA1 region of the hippocampus in these mouse cohorts confirmed that pSer129–α-synuclein staining was seen only in mice overexpressing human α-synuclein (Fig. 4 *A* and *D*). Significantly, 110A53T mice showed decreased pSer129–α-synuclein levels relative to A53T mice (Fig. 4 *A* and *D*; 286.46 ± 21 versus 206.43 ± 24; $P < 0.01$), indicating that Hsp110 overexpression can indeed decrease fibrillization of α-synuclein in vivo in the context of a disease model. Imaging performed at 9 mo reveals similar patterns in Hsp110 and pSer129–α-synuclein levels among transgenics (*SI Appendix*, Fig. S3). The Hsp110 disaggregase is known to both fragment and depolymerize α-synuclein fibrils in vitro. Therefore, we tested for α-synuclein oligomer content using an antibody that can recognize this α-synuclein species. Interestingly, we did not

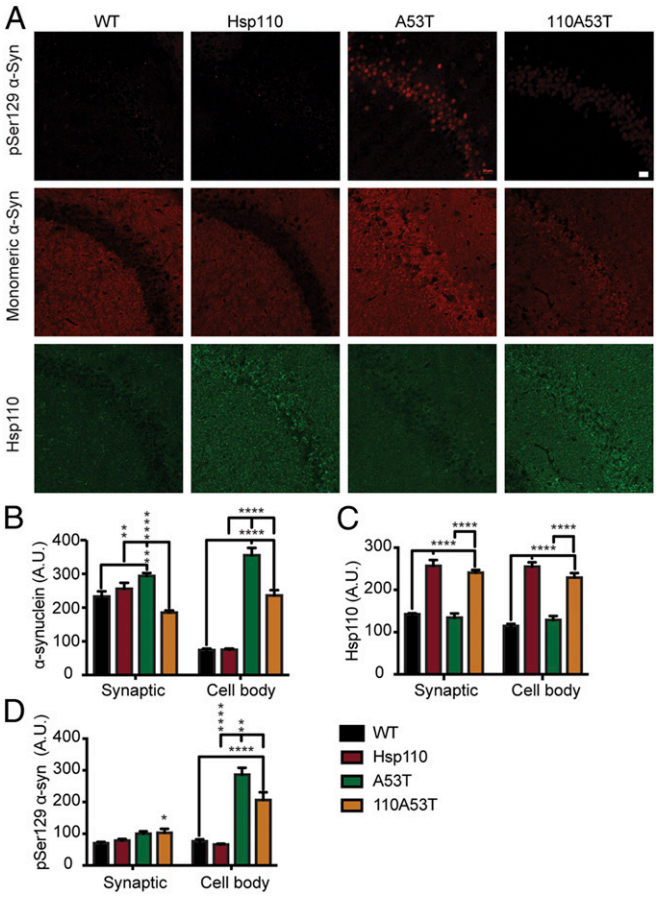

Fig. 4. Characterization of α-synuclein pathology in 110A53T brains. (*A*) Representative fluorescence images of 6-mo-old WT, Hsp110, A53T, and 110A53T mouse CA1 of hippocampus. First row of images: pSer129–α-synuclein in red; second row, total α-synuclein in red; and third row, Hsp110 in green. (Scale bar, 20 μm, applies to all panels.) (*B*) Quantification of total α-synuclein levels in cell body layer as well as synaptic regions; $n = 3$ mice per genotype. (*C*) Quantification of Hsp110 levels in cell body layer and in synaptic regions; $n = 3$ mice per genotype. (*D*) Quantification of pSer129–α-synuclein levels in cell body layer and in synaptic regions, $n = 3$ mice per genotype. Data were analyzed by ANOVA; *P value < 0.05; **P value < 0.01; ****P value < 0.0001.

observe a change in oligomeric α-synuclein levels (*SI Appendix*, Fig. S4) in 110A53T mice relative to A53T mice, suggesting that the fibrils were being broken down completely or that Hsp110 overexpression is preventing the formation of oligomers and fibrils.

We then performed immunostaining in spinal cord sections of the 6-mo-old mouse cohort. Due to the different fixation process that we used for spinal cord, we were unable to detect pSer129–α-synuclein staining in motor neurons from any of these strains. As noted above for the brain sections, however, we did not observe a significant decrease in oligomeric α-synuclein levels (*SI Appendix*, Fig. S5 *C* and *D*; P value = 0.088) or total α-synuclein levels (*SI Appendix*, Fig. S5 *A* and *B*; P value = 0.141) in motor neurons of 110A53T mice relative to A53T mice, even though there was a tendency for decreases for both species in 110A53T spinal cords. The immunohistochemistry results suggest that Hsp110 overexpression primarily acts to decrease fibrillized α-synuclein levels. These results also indicate that Hsp110 is not disaggregating α-synuclein fibrils into oligomers.

Finally, we tested if Hsp110 overexpression improves survival because of the decreased α-synuclein pathology. Kaplan–Meier analysis shows that 110A53T mice have increased survival compared to their A53T littermates (*SI Appendix*, Fig. S6; 50% survival for A53T is 250 d versus 110A53T survival of 300 d; $P = 0.03$). Collectively, these findings suggest that Hsp110 overexpression is capable of mitigating α-synuclein aggregative pathology and increasing survival.

Hsp110 Transgenic Mice Show Limited Spread of α-Synuclein Pathology When Injected with Preformed Fibrils. Braak staging of PD suggests that α-synuclein pathology spreads in a temporally and spatially predictable manner to affect the substantia nigra and eventually the cortex (44). The regions affected mirror the course of the disease and associated symptoms. To follow the spread of α-synuclein in vivo, we recombinantly expressed, purified, and aggregated α-synuclein preformed fibrils (PFFs) and injected these unilaterally into the dorsal striatum of WT and Hsp110 mice (7 mo old). The mice were perfused 6 wk later to evaluate spread of pathology to the substantia nigra, basolateral amygdala, and motor cortex by immunostaining for pSer129–α-synuclein. The abundance of pSer129–α-synuclein pathology in the substantia nigra pars compacta, basolateral amygdala, and motor cortex was scored. Hsp110 overexpression dramatically decreased α-synuclein pathology in all 3 areas (Fig. 5). Quantification of pSer129–α-synuclein in tyrosine hydroxylase-positive regions of the substantia nigra showed an ∼5-fold decrease in the abundance of pSer129–α-synuclein inclusion in Hsp110 transgenic mice (WT: 5.31 ± 2.52 A.U.; Hsp110: 1.00 ± 0.87 A.U.; $P < 0.01$). Similar results were found in both the basolateral amygdala and motor cortex; quantification of pSer129–α-synuclein resulted in an ∼3-fold decrease in α-synuclein pathology in the basolateral amygdala of Hsp110 transgenic mice (WT: 2.91 ± 0.32 A.U.; Hsp110: 1.00 ± 0.38 A.U.; $P < 0.01$) and an ∼2.5-fold decrease in α-synuclein pathology in the motor cortex of Hsp110 transgenic mice (WT: 2.71 ± 0.48 A.U.; Hsp110: 1.00 ± 0.22 A.U.; $P < 0.01$). Interestingly, quantification of pSer129–α-synuclein at the striatum showed no difference between WT and Hsp110 transgenic mice, indicating that the initial PFF levels were equivalent and that Hsp110 is effective in ameliorating the spread of α-synuclein pathology throughout the brain from the injection site.

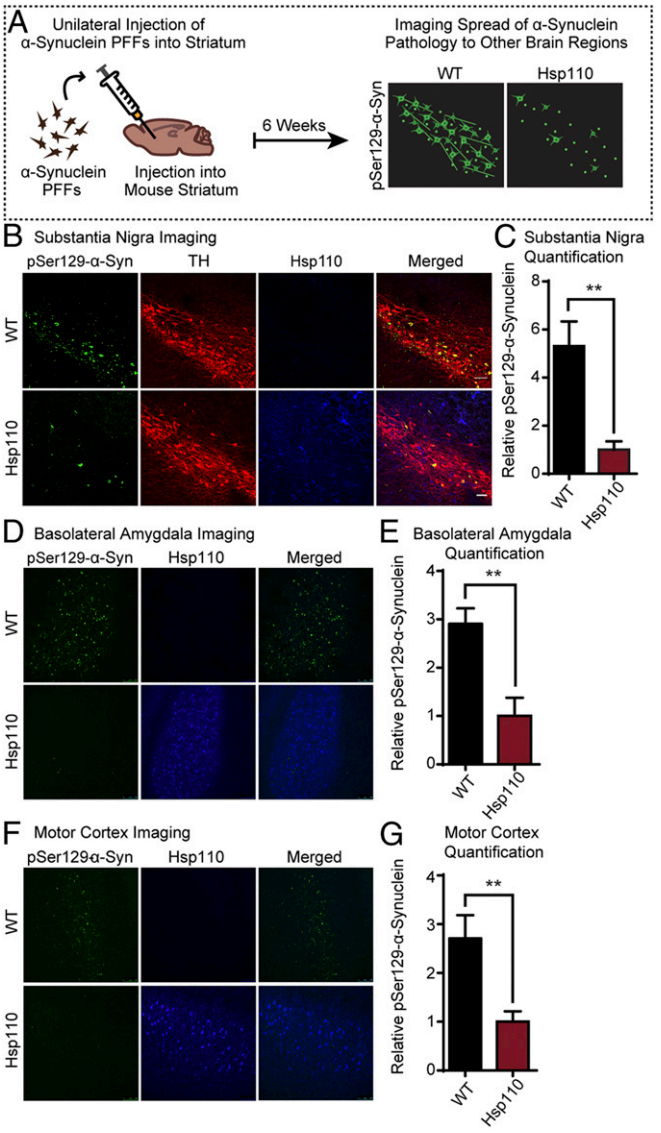

Fig. 5. Transgenic expression of Hsp110 mitigates the spread of injected α-synuclein PFFs. (*A*) Schematic showing stereotaxic brain injections of α-synuclein PFFs and subsequent imaging. WT and Hsp110 mice were injected with α-synuclein PFFs into the striatum at 7 mo of age. After 6 wk, the mice were perfused, and the substantia nigra was imaged for the presence of pSer129–α-synuclein, indicating spread of pathology from the striatum. (*B*) Representative images of WT and Hsp110 mouse substantia nigra 6 wk postinjection, with pSer129–α-synuclein stained in green, tyrosine hydroxylase (TH) stained in red, and Hsp110 in blue. (*C*) Quantitation of pSer129–α-synuclein levels in WT and Hsp110 mouse substantia nigra. $n = 6$ mice/genotype; $^{**}P < 0.01$, Student's t test. (*D*) Representative images of WT and Hsp110 mouse basolateral amygdala 6 wk postinjection with pSer129–α-synuclein stained in green and Hsp110 in blue. (*E*) Quantitation of pSer129–α-synuclein levels in WT and Hsp110 mouse basolateral amygdala. $n = 6$ or 7 mice/genotype; $^{**}P < 0.01$, Student's t test. (*F*) Representative images of WT and Hsp110 mouse motor cortex 6 wk postinjection, with pSer129–α-synuclein stained in green and Hsp110 in blue. (*G*) Quantitation of pSer129–α-synuclein levels in WT and Hsp110 mouse motor cortex. (Scale bar, 50 μm, and applies to all panels in *A*, *B*, *D*, and *F*.) $n = 6$ or 7 mice/genotype; $^{**}P < 0.01$, Student's t test.

Discussion

In this study, we demonstrate that enhancing the potential disaggregase capacity by increasing Hsp110 levels mitigates α-synuclein pathology. We show that overexpressing Hsp110 (2- to 4-fold; Figs. 1 and 2) is effective in decreasing α-synuclein aggregation both in cell culture (Fig. 1) and in 2 distinct mouse models of α-synucleinopathy (Figs. 4 and 5 and *SI Appendix*, Fig. S1). Our work strongly supports the hypothesis that Hsp110 acts to counter α-synuclein aggregation in vivo. This is in line with prior proteomic characterization of Lewy bodies that found that these hallmarks of α-synuclein aggregative pathology were enriched in chaperone components (45). In the transgenic model, there is a gradual accretion of α-synuclein aggregates with the formation of pSer129–α-synuclein–positive pathology (Fig. 4), while in the PFF model,

synthetic fibrils were injected to induce endogenous protein to form pSer129-positive pathologic inclusions (Fig. 5). In both models, Hsp110 was effective in reducing observed pathology as much as 5-fold, suggesting that Hsp110 can act on a wide variety of α-synuclein fibrillar species. Through staining for pathogenic oligomeric α-synuclein species, we confirmed that the α-synuclein fibrils were disaggregated completely (*SI Appendix*, Fig. S3). This is congruent with survival findings that 110A53T mice have an increased survival compared to A53T (*SI Appendix*, Fig. S6). This indicates either that the disaggregase is breaking down α-synuclein fibrils into monomers or that elevated Hsp110 levels are effective in preventing the misfolding and templating of α-synuclein.

Our findings suggest that Hsp110 overexpression is a potential strategy not only to increase disaggregase activity but chaperone capacity more broadly (Fig. 3). The unbiased mass spectrometry comparing WT and Hsp110 showed that several Hsp70s and DnaJs were increased at nerve termini—the site of initiation of α-synuclein aggregation (46). The increased chaperone capacity should counter not only α-synuclein aggregation but also its negative effects on synaptic vesicle cycling and neuronal dysfunction (47). Hsp110 has been linked to many chaperone activities, and these should be broadly beneficial for synaptic proteostasis. Hsp110, through its NEF activity, is expected to support synaptic vesicle endocytosis and enhance synaptic vesicle cycling. We plan to test this premise in the future. While our experiments reach a consensus that overexpression of Hsp110 is helpful overall, they also suggest that there is a threshold, and that going beyond 2-fold might lead to greater benefit. The alternative strategy of enhancing disaggregase activity by increasing DnaJB1 appears to be effective in a Huntington model (32). Therefore, dual overexpression of these 2 disaggregase components is worth testing for therapeutic efficacy.

Our results add to the growing body of work establishing the relevance of the disaggregase in ameliorating neurodegenerative diseases. This has been confirmed by knockdowns to the disaggregase components, which increased aggregation of disease-relevant proteins such as polyQ (32) in *Caenorhabditis elegans* and tau in mice (33). Previous work from the A.L.H. laboratory has shown that Hsp110 overexpression can increase median survival by 2 mo in an ALS model (31). Therefore, we suggest the need to screen for small molecules that increase Hsp110 expression. These molecules could be tested as therapeutics for both intracellular α-synuclein aggregation and prion-like spread.

Materials and Methods

For a detailed description of materials and methods, see *SI Appendix, Materials and Methods*.

Mice. All experiments with animals were approved by the Institutional Animal Care and Use Committee at Yale University or University of Alabama, Birmingham.

HEK293T Overexpression and Fibril Assay. HEK293T aggregation assay was completed as described in Taguchi et al. (36). HEK293T cells were transfected with human α-synuclein–GFP (AddGene 40822), empty pCAG vector, and/or CAG-driven human Hsp110 cDNA [HspA4L (Apg1, HSPH3, isoform1)]. Oligomeric α-synuclein (0.2 mg/mL) was used to seed intracellular aggregation. Quantitation of the percentage of cells with aggregates was completed manually through random visualization of ≥100 cells per replicate.

Mass Spectrometric Analysis. Synaptosomes of the denoted genotypes were prepared as described previously (48). LFQ of these samples was done on a Thermo Fusion Orbitrap as previously described (49). Proteins with at least 2 independent peptides were analyzed after normalizing to both spiked internal standards and total spectral counts. Pathways altered in the 4 genotypes were identified using STRING analysis.

Purification of α-Synuclein and Generation of PFFs. Expression of α-synuclein in BL21 cells and purification was performed as described (50). Fibrils were generated by shaking 350 μM (5 mg/mL) α-synuclein for 7 d in 50 mM Tris·HCl, pH 7.5, and 150 mM KCL (51).

Stereotaxic Injections and Imaging of α-Synuclein Spread. At 7 mo of age, Hsp110 transgenic mice and littermate controls were anesthetized and stereotactically injected with 2 μL of 5 mg/mL of sonicated fibrils into the right striatum or 2 μL of 5 mg/mL monomeric α-synuclein (52). Coordinates were 1.0 mm posterior, 2.0 mm lateral, and −3.2 mm ventral. Six weeks after injections, mice were transcardially perfused. Sections were analyzed by immunohistochemistry with the following antibodies: anti-pS129–α-synuclein (53), tyrosine hydroxylase (1:1,000), and Hsp110 (1:100). The phosphorylated p-S129–α-synuclein in all brain regions was quantified using Image J. Analysis was done blind to genotype.

Data Availability. Mass spectrometry data have been deposited in the PRIDE database.

ACKNOWLEDGMENTS. We thank John Lee for mouse husbandry, genotyping, and survival analysis. We thank TuKiet Lam for mass spectrometry assistance. This work was supported by NIH Grants R01NS083846 and R01NS110354 (to S.S.C.) and Grant 1R01NS102257 (to L.V.-D.); the Nina Compagnon Hirshfield Parkinson's Disease Research Fund and Congressionally Directed Medical Research Programs Award W81XWH-17-1-0564 (to S.S.C.); and the Michael J. Fox Foundation (L.V.-D.). A.L.H. is supported by the Howard Hughes Medical Institute. Y.V.T. is a recipient of the Lo Graduate Fellowship for Excellence in Stem Cell Research. Y.V.T. and E.L.G. were supported by the National Institute of Neurological Disorders and Stroke T32 "Neurobiology of Cortical Systems" NS007224 training grant. E.L.G. was also supported by Interdepartmental Neuroscience Program Grant T32 NS041228 and the Gruber Foundation. Mass spectrometric experiments were done with support from the Yale/National Institute on Drug Abuse Neuroproteomic Center (P30 DA018343) and instrumentation was obtained with a National Institutes of Health Shared Instrumentation Grant (S10OD018034).

1. R. L. Nussbaum, C. E. Ellis, Alzheimer's disease and Parkinson's disease. *N. Engl. J. Med.* **348**, 1356–1364 (2003).
2. S. Chandra, X. Chen, J. Rizo, R. Jahn, T. C. Südhof, A broken alpha-helix in folded alpha-synuclein. *J. Biol. Chem.* **278**, 15313–15318 (2003).
3. K. J. Vargas *et al.*, Synucleins regulate the kinetics of synaptic vesicle endocytosis. *J. Neurosci.* **34**, 9364–9376 (2014).
4. V. M. Nemani *et al.*, Increased expression of alpha-synuclein reduces neurotransmitter release by inhibiting synaptic vesicle reclustering after endocytosis. *Neuron* **65**, 66–79 (2010).
5. J. Burré *et al.*, Alpha-synuclein promotes SNARE-complex assembly in vivo and in vitro. *Science* **329**, 1663–1667 (2010).
6. M. G. Spillantini *et al.*, Alpha-synuclein in Lewy bodies. *Nature* **388**, 839–840 (1997).
7. R. Krüger *et al.*, Ala30Pro mutation in the gene encoding alpha-synuclein in Parkinson's disease. *Nat. Genet.* **18**, 106–108 (1998).
8. S. Lesage *et al.*; French Parkinson's Disease Genetics Study Group, G51D α-synuclein mutation causes a novel parkinsonian-pyramidal syndrome. *Ann. Neurol.* **73**, 459–471 (2013).
9. M. H. Polymeropoulos *et al.*, Mutation in the alpha-synuclein gene identified in families with Parkinson's disease. *Science* **276**, 2045–2047 (1997).
10. C. Proukakis *et al.*, A novel α-synuclein missense mutation in Parkinson disease. *Neurology* **80**, 1062–1064 (2013).
11. J. J. Zarranz *et al.*, The new mutation, E46K, of alpha-synuclein causes Parkinson and Lewy body dementia. *Ann. Neurol.* **55**, 164–173 (2004).
12. P. Pasanen *et al.*, Novel α-synuclein mutation A53E associated with atypical multiple system atrophy and Parkinson's disease-type pathology. *Neurobiol. Aging* **35**, 2180.e1–2180.e5 (2014).
13. M. C. Chartier-Harlin *et al.*, Alpha-synuclein locus duplication as a cause of familial Parkinson's disease. *Lancet* **364**, 1167–1169 (2004).
14. A. B. Singleton *et al.*, α-Synuclein locus triplication causes Parkinson's disease. *Science* **302**, 841 (2003).
15. B. Bukau, A. L. Horwich, The Hsp70 and Hsp60 chaperone machines. *Cell* **92**, 351–366 (1998).
16. S. Rüdiger, A. Buchberger, B. Bukau, Interaction of Hsp70 chaperones with substrates. *Nat. Struct. Biol.* **4**, 342–349 (1997).
17. A. Szabo *et al.*, The ATP hydrolysis-dependent reaction cycle of the Escherichia coli Hsp70 system DnaK, DnaJ, and GrpE. *Proc. Natl. Acad. Sci. U.S.A.* **91**, 10345–10349 (1994).
18. P. J. Dekker, N. Pfanner, Role of mitochondrial GrpE and phosphate in the ATPase cycle of matrix Hsp70. *J. Mol. Biol.* **270**, 321–327 (1997).
19. K. Liberek, J. Marszalek, D. Ang, C. Georgopoulos, M. Zylicz, Escherichia coli DnaJ and GrpE heat shock proteins jointly stimulate ATPase activity of DnaK. *Proc. Natl. Acad. Sci. U.S.A.* **88**, 2874–2878 (1991).
20. J. S. McCarty, A. Buchberger, J. Reinstein, B. Bukau, The role of ATP in the functional cycle of the DnaK chaperone system. *J. Mol. Biol.* **249**, 126–137 (1995).
21. T. Langer *et al.*, Successive action of DnaK, DnaJ and GroEL along the pathway of chaperone-mediated protein folding. *Nature* **356**, 683–689 (1992).

22. D. Wall, M. Zylicz, C. Georgopoulos, The NH2-terminal 108 amino acids of the Escherichia coli DnaJ protein stimulate the ATPase activity of DnaK and are sufficient for lambda replication. *J. Biol. Chem.* **269**, 5446–5451 (1994).
23. N. B. Nillegoda *et al*., Crucial HSP70 co-chaperone complex unlocks metazoan protein disaggregation. *Nature* **524**, 247–251 (2015).
24. H. Rampelt *et al*., Metazoan Hsp70 machines use Hsp110 to power protein disaggregation. *EMBO J.* **31**, 4221–4235 (2012).
25. M. E. Desantis, J. Shorter, The elusive middle domain of Hsp104 and ClpB: Location and function. *Biochim. Biophys. Acta* **1823**, 29–39 (2012).
26. X. Gao *et al*., Human Hsp70 disaggregase reverses Parkinson's-linked α-synuclein amyloid fibrils. *Mol. Cell* **59**, 781–793 (2015).
27. C. Andréasson, J. Fiaux, H. Rampelt, M. P. Mayer, B. Bukau, Hsp110 is a nucleotide-activated exchange factor for Hsp70. *J. Biol. Chem.* **283**, 8877–8884 (2008).
28. Z. Dragovic, S. A. Broadley, Y. Shomura, A. Bracher, F. U. Hartl, Molecular chaperones of the Hsp110 family act as nucleotide exchange factors of Hsp70s. *EMBO J.* **25**, 2519–2528 (2006).
29. H. Raviol, H. Sadlish, F. Rodriguez, M. P. Mayer, B. Bukau, Chaperone network in the yeast cytosol: Hsp110 is revealed as an Hsp70 nucleotide exchange factor. *EMBO J.* **25**, 2510–2518 (2006).
30. U. Bandyopadhyay *et al*., RNA-Seq profiling of spinal cord motor neurons from a presymptomatic SOD1 ALS mouse. *PLoS One* **8**, e53575 (2013).
31. M. Nagy, W. A. Fenton, D. Li, K. Furtak, A. L. Horwich, Extended survival of misfolded G85R SOD1-linked ALS mice by transgenic expression of chaperone Hsp110. *Proc. Natl. Acad. Sci. U.S.A.* **113**, 5424–5428 (2016).
32. A. Scior *et al*., Complete suppression of Htt fibrilization and disaggregation of Htt fibrils by a trimeric chaperone complex. *EMBO J.* **37**, 282–299 (2018).
33. B. Eroglu, D. Moskophidis, N. F. Mivechi, Loss of Hsp110 leads to age-dependent tau hyperphosphorylation and early accumulation of insoluble amyloid beta. *Mol. Cell. Biol.* **30**, 4626–4643 (2010).
34. L. Ping *et al*., Global quantitative analysis of the human brain proteome in Alzheimer's and Parkinson's disease. *Sci. Data* **5**, 180036 (2018).
35. K. C. Luk *et al*., Exogenous alpha-synuclein fibrils seed the formation of Lewy body-like intracellular inclusions in cultured cells. *Proc. Natl. Acad. Sci. U.S.A.* **106**, 20051–20056 (2009).
36. Y. V. Taguchi *et al*., Glucosylsphingosine promotes α-synuclein pathology in mutant GBA-associated Parkinson's disease. *J. Neurosci.* **37**, 9617–9631 (2017).
37. L. Maroteaux, J. T. Campanelli, R. H. Scheller, Synuclein: A neuron-specific protein localized to the nucleus and presynaptic nerve terminal. *J. Neurosci.* **8**, 2804–2815 (1988).
38. X. Lin *et al*., Leucine-rich repeat kinase 2 regulates the progression of neuropathology induced by Parkinson's-disease-related mutant α-synuclein. *Neuron* **64**, 807–827 (2009).
39. S. Chandra, G. Gallardo, R. Fernández-Chacón, O. M. Schlüter, T. C. Südhof, Alpha-synuclein cooperates with CSPalpha in preventing neurodegeneration. *Cell* **123**, 383–396 (2005).
40. L. Fourgeaud *et al*., TAM receptors regulate multiple features of microglial physiology. *Nature* **532**, 240–244 (2016).
41. G. Gallardo, O. M. Schlüter, T. C. Südhof, A molecular pathway of neurodegeneration linking alpha-synuclein to ApoE and Abeta peptides. *Nat. Neurosci.* **11**, 301–308 (2008).
42. J. P. Anderson *et al*., Phosphorylation of Ser-129 is the dominant pathological modification of alpha-synuclein in familial and sporadic Lewy body disease. *J. Biol. Chem.* **281**, 29739–29752 (2006).
43. H. Fujiwara *et al*., α-Synuclein is phosphorylated in synucleinopathy lesions. *Nat. Cell Biol.* **4**, 160–164 (2002).
44. H. Braak *et al*., Staging of brain pathology related to sporadic Parkinson's disease. *Neurobiol. Aging* **24**, 197–211 (2003).
45. J. B. Leverenz *et al*., Proteomic identification of novel proteins in cortical Lewy bodies. *Brain Pathol.* **17**, 139–145 (2007).
46. M. L. Kramer, W. J. Schulz-Schaeffer, Presynaptic alpha-synuclein aggregates, not Lewy bodies, cause neurodegeneration in dementia with Lewy bodies. *J. Neurosci.* **27**, 1405–1410 (2007).
47. J. M. Froula *et al*., α-Synuclein fibril-induced paradoxical structural and functional defects in hippocampal neurons. *Acta Neuropathol. Commun.* **6**, 35 (2018).
48. C. H. Westphal, S. S. Chandra, Monomeric synucleins generate membrane curvature. *J. Biol. Chem.* **288**, 1829–1840 (2013).
49. M. X. Henderson *et al*., Neuronal ceroid lipofuscinosis with DNAJC5/CSPα mutation has PPT1 pathology and exhibit aberrant protein palmitoylation. *Acta Neuropathol.* **131**, 621–637 (2016).
50. L. A. Volpicelli-Daley, K. C. Luk, V. M. Lee, Addition of exogenous α-synuclein preformed fibrils to primary neuronal cultures to seed recruitment of endogenous α-synuclein to Lewy body and Lewy neurite-like aggregates. *Nat. Protoc.* **9**, 2135–2146 (2014).
51. L. Bousset *et al*., Structural and functional characterization of two alpha-synuclein strains. *Nat. Commun.* **4**, 2575 (2013).
52. K. C. Luk *et al*., Pathological α-synuclein transmission initiates Parkinson-like neurodegeneration in nontransgenic mice. *Science* **338**, 949–953 (2012).
53. N. J. Rutherford, M. Brooks, B. I. Giasson, Novel antibodies to phosphorylated α-synuclein serine 129 and NFL serine 473 demonstrate the close molecular homology of these epitopes. *Acta Neuropathol. Commun.* **4**, 80 (2016).